A study of different cloud detection methods for the JEM-EUSO atmospheric monitoring system

A. ANZALONE[1], M. BERTAINA[2], R. CREMONINI[2], M.D. FRÍAS RODRÍGUEZ[3], F. ISGRÓ[4] FOR THE JEM-EUSO COLLABORATION

[1]INAF-IASF, Palermo, Italy

[2]Dipartimento di Fisica, Universitá degli Studi di Torino, Italy

[3]SPACE & AStroparticle (SPAS) Group, UAH, Madrid, Spain

[4]Dipartimento di Scienze Fisiche, Universitá degli Studi di Napoli Federico II, Italy

anna.anzalone@ifc.inaf.it

Abstract: The observation of the atmosphere is a crucial task for the JEM-EUSO mission, and a module for the atmospheric monitoring is included in the design of the whole system. In this paper the retrieval of cloud coverage in the field of view of the telescope is addressed considering both radiative methods commonly used in the meteorological field and methods of image analysis, with the aim of studying the feasibility of these approaches to the data that the JEM-EUSO infra red camera will provide. The complementarity of the two approaches will be further investigated, together with a different set of techniques, to contribute to achieve the best cloud estimation in JEM-EUSO.

Keywords: JEM-EUSO experiment, atmospheric monitoring system, cloud detection, cloud height.

1 Introduction

The strength of the fluorescent light and the Cherenkov signal received from EAS, as well as the reconstruction efficiency and errors, depend on the transparency of the atmosphere, the cloud coverage and the height of the cloud top. A crucial task for the success of the JEM-EUSO mission [1] is to observe the conditions of the atmosphere in the field of view of the telescope. To this end a dedicated atmospheric monitoring (AM) system [2] is being designed. The system includes an infrared camera, that will be used to estimate cloudiness and height maps in the field of view of the telescope.

This paper reports on current work to identify optimal cloud detection algorithms from infrared data, that will be implemented into the JEM-EUSO observing system for accurate estimations of cosmic-ray energy. To this end here we revise the performance of different methods for cloud detection: threshold algorithms, radiative, and methods exploiting image analysis techniques. The experiments are run on scenes under different conditions, retrieved by operational atmospheric sensors similar to the JEM-EUSO atmospheric monitoring system.

2 Radiative methods

Geostationary (i.e. GOES, MSG) and LEO satellites (i..e. Terra/Aqua, HIRS) provide multi-spectral observations with good spatial and temporal resolution. CALIPSO mission combines an active lidar instrument with passive infrared and visible images to probe the vertical structure and properties of thin clouds and aerosols over the globe. The cloud mask (CMa) allows the identification of cloud free areas where other products (total or layer precipitable water, stability analysis imagery, snow/ice cover delineation) may be computed. The main aim of the CMa is therefore to delineate all cloud-free pixels in a satellite scene with a high confidence. In addition, the typical CMa product provides information on the presence of snow/sea ice, dust clouds and volcanic plumes. SEVIRI is a multi-band sensors operating on MSG satellite series by EUMETSAT [12]: starting from SERIVI radiance observations, it has been developed an algorithm for identifying cloud presence and cloud contamination. The algorithm is based on several and differential band threshold tests, using only infra red bands as JEM-EUSO work during nighttime: some difference band tests are specific for thin cirrus detection. Thresholds depend on pixel background (land, water and coast) and on Numerical Weather Prediction (NWP) model temperature at surface and at standard levels. Starting from four categories
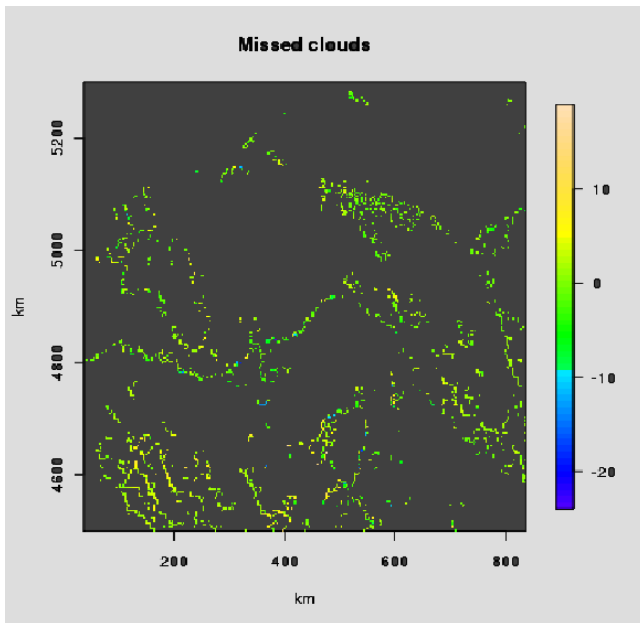
Figure 1: Single IR band cloud detection respect all IR channel CMa

Figure 2: Band difference from SEVIRI for 10.8 μm and 12.0 μm at 12:45 on 2th sept 2010

of tests a probability of clear sky is defined as follow:

$$cloud\,sky\,probability = \sqrt[3]{P_{ir} \cdot P_{thin} \cdot P_{diff-ir}}$$

Where P_{ir} test is the probability that for a given band/threshold the pixel is cloudy or cloud contaminated; P_{thin} and $P_{diff-ir}$ have the same meaning but for band differences and thin cirrus specific tests. As JEM-EUSO will work with at least with a two band infrared camera, the tests performed on SEVIRI have been limited to 10.8 and 12.0 μm bands. Single infrared algorithm can detect only thick and extended clouds, with better performance during summer and over warm sea due to high thermal contrast [10].

Figure 1 shows undetected clouds when only 10.8 μm IR band is used: major problems occur near coastal border-line, with thin cirrus and at border of cloud desk, where pixels and not fulfilled. Well-known split window channels are essential to detect thin cirrus or broken clouds and to estimate Earth's surface and cloud top temperatures. The 12.0 μm band is more sensitive for high thin cirrus but it is not easy to recognise through visual inspection, while it is highlighted by band difference [11].

Figure 2 shows the difference between Brightness Temperature (BT) at 10.8 μm and 12.0 μm at 12:45 on 2th sept 2010: BT differences greater than $3^\circ K$ distinguish between semi-transparent thin clouds and thick ones.
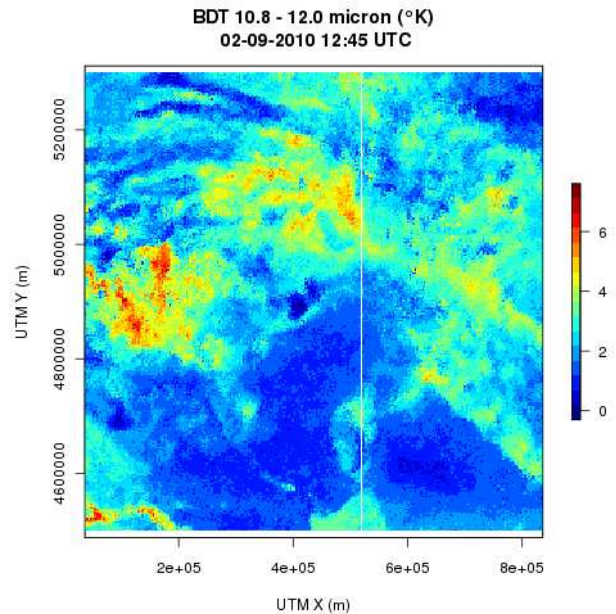
3 Image analysis methods

The methods discussed in this Section exploit the image content of the infrared data, not considering its physical meaning. That is that the content of a pixel is regarded as a colour information only, and not as related to the temperature.

In this Section we consider two different methods: a supervised image segmentation algorithm, and a second method that follows a geometric approach.

3.1 Feature based method

In this method the classification of the cloudy pixels is performed using a state of the art machine learning tool: a Support Vector Machine (SVM) [6], for which we chose a Gaussian kernel. In particular we use a public available implementation of the SVM [5].

The classification using SVM is a supervised method, and it needs a training set of data. This means that a relatively large number of pixels must be manually labelled. A simple graphical interface has been created to facilitate this task.

The classification is not performed in the gray-level space, but each image pixel is mapped into a higher dimensional space, that is usually called feature space. In our case the feature vector associated to each pixel (i,j) is

$$\mathbf{f_{i,j}} = (v, \mu, \sigma, D_x, D_y, h_1, h_2, h_3, h_4, h_5, h_6, h_7, h_8)$$

where v is the gray-level of pixel (i,j), μ and σ are mean and standard deviation respectively in a 5×5 neighbourhood centred in the pixel, D_x and D_y are the gradient

components, and h_1 to h_8 are the entities of the eight-bin histogram of the 5×5 neighbourhood in the image.

The classifier has been tested on more than 2000 images from different sensors. The training set includes 610 points belonging to both *cloud* and *not-cloud* classes, manually selected from the first 1000 frames of the image set. From the remainder of the sequence we selected further 609 points that have been used as test set for evaluating the performance of the classifier. As it can be seen from the ROC curve shown in Figure 3 the performances are particularly good, since the test set is temporally close to the training set. We are planning to use more data for a better evaluation.
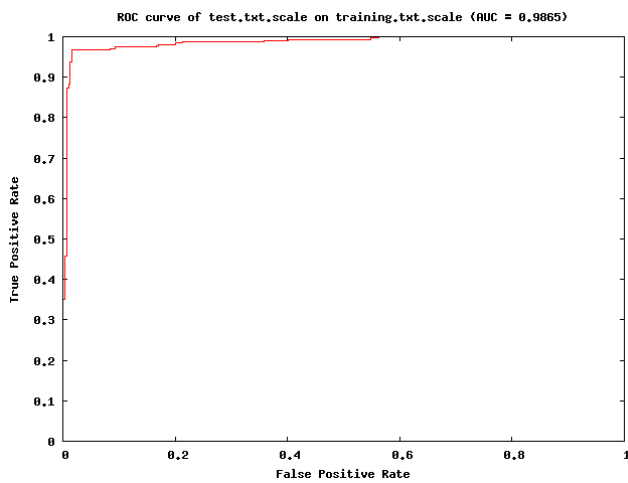

Figure 3: ROC curve for the SVM classifier.

3.2 Stereo based method

In this section the possibility of retrieving maps of cloudiness from maps of heights is presented supposing that stereo acquisition was enabled by the use of the infra red camera. Using stereo methods, the depth of the imaged points can be recovered from two, or more, images, in this way, in presence of clouds, the cloud-top height (CTH) can be recovered [8, 7, 4]. Stereo could be achieved in JEM-EUSO exploiting the ISS movement. While the ISS flies along its orbit, the IR camera acquires an image of the FoV at every fixed time interval.

Exploiting this information, and the fact that the images can be geo-located, we can mark as clouds all those pixels for which the recovered height is higher than the altitude of the corresponding ground.

We analyse the feasibility of this method studying the theoretical reconstruction error for the depth, as a large error in reconstruction may lead, especially for lower clouds, to mis-classification.
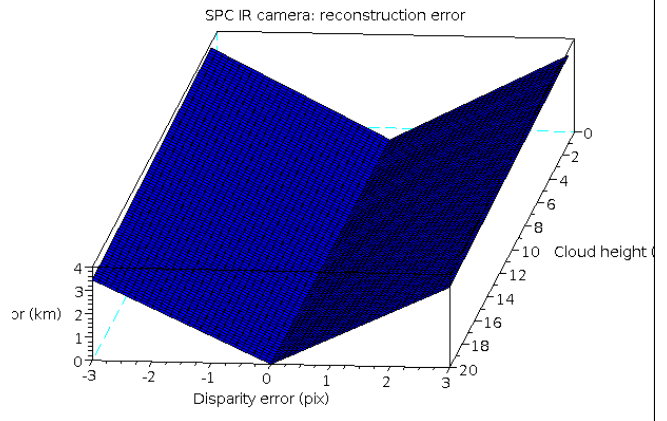

Figure 4: Plot of the CTH estimate error against the disparity error and the true CTH. ISS station altitude at 430 Km.

The depth Z of a point can be obtained by triangulation as

$$\hat{Z} = \frac{b}{\hat{d}_x}$$

where b is the baseline of the stereo system (the distance covered by the ISS between the two views), and $\hat{d}_x$ is the estimated disparity [9]. If d_x and Z are the true disparity and the true depth respectively we have that

$$\hat{d}_x = d_x + \delta x$$

and

$$Z = \frac{b}{d_x}$$

We can write the depth error δZ as a function of δx by Taylor expansion as

$$\delta Z = \frac{b}{d_x^2} \delta x = \frac{Z^2}{b} \delta x$$

which shows that for a fixed baseline b and δx then the error in the depth measurement rises as the square of distance from the camera. Therefore we need a large baseline b to get a good depth resolution, but also we can expect a poor depth resolution for distant objects.

The error function is plotted in Figure 4. For this simulation we used the specs for the infrared camera given in Table 1, the altitude of the sensor fixed at 430 Km, and a time interval between the two images of 32 sec, which ensures a 50% overlap.

From the analysis of the results of the simulations we can conclude that we have an accuracy within 500 meters with a disparity error of 0.5 pixels, that can be achieved for most pixels with a good matching strategy. With higher disparity error, say 1-2 pixels, we have an error in the depth estimation that is within 2 Km.

	FoV	IFoV	Pixel resolution	Number of of pixels	Focal length	Pixel pitch
	60°	0.1°		640×480	15 mm	20μm
ISS$_h$=350 Km			$\simeq 0.58$ Km			
ISS$_h$=430 Km			$\simeq 0.72$ Km			

Table 1: Specification for the IR camera used for this experiment

4 Conclusions

Radiative and image methods for cloud detection and cloud height estimation have been preliminary considered as candidates for JEM-EUSO atmospheric monitoring system. While performance of radiative methods depend on IR camera thermal resolution and available bands - especially when the scene is thin cirrus contaminated - the image methods described in this contribution depend on spatial angular resolution of the sensors, and on the quality of the features or on the quality of the matching. Both radiative and image methods need to be deeper investigated and moreover other well known techniques and features in image analysis will be investigated. Radiative and image approaches can be considered as complementary, an their integration to best achieve cloud coverage estimation for JEM-EUSO will be considered.

References

[1] T. Ebisuzaki et al.: 2011, The JEM-EUSO mission, 32nd ICRC (ID1628)

[2] A. Neronov et. al: 2011, Atmospheric Monitoring System of JEM-EUSO, 32nd ICRC (ID301)

[3] J.A. Morales et. al.: 2011, The IR-Camera of the JEM-EUSO (JAXA) Space Observatory, 32nd ICRC (ID1031)

[4] Anzalone A. et al.: 2004, Proceedings of MDIC04, 75-86

[5] Chih-Chung Chang et al.: LIBSVM:a library for support vector machines, 2001 http://www.csie.ntu.edu.tw/~cjlin/libsvm

[6] Shawe-Taylor J. et al.: 2000, Support Vector Machines and other kernel-based learning methods. Cambridge University Press

[7] J.P. Muller et al.: 2007, Journal of Applied Meteorology and Climatology, International Journal of Remote Sensing, **28**(9), 1921-1938

[8] G. Seiz et al: 2006, Journal of Applied Meteorology and Climatology, 2006, **46**, 1182-1195

[9] E. Trucco and A. Verri: 1998, Introductory Techniques for 3-D Computer Vision, Prentice Hall

[10] Stanley Q., Kidder and Thomas H. Vonder Haar., San Diego, CA: Academic Press, **1995**.

[11] Krebs, W. Mannstein, H., Bugliaro, L., and Mayer, B., Atmos. Chem. Phys., 2007, **Volume**(7): 6145,6159

[12] Schmid, J., **1999**, available at http://www.eumetsat.int